15 November 1999
PHYSICS LETTERS A
ELSEVIER
Physics Letters A 262 (1999) 457–463
www.elsevier.nl/locate/physleta

Generation of X-rays due to multiple runaway breakdown inside thunderclouds

A.V. Gurevich [a,*], G.M. Milikh [b]

[a] P.N. Lebedev Institute of Physics, Moscow 117924, Russia
[b] Department of Astronomy, University of Maryland, College Park, MD 20742, USA

Received 3 September 1999; accepted 15 September 1999
Communicated by V.M. Agranovich

Abstract

Generation of X-rays due to multiple runaway breakdown inside thunderclouds is discussed. The model is based on the recently developed kinetic theory of the runaway breakdown, and detailed theory of the X-rays propagation in the atmosphere from the source to detector, which is determined by the Compton scattering. The model is shown to be in qualitative agreement with observations of the X-ray spectrum. A comparison with the observed electric field distribution and X-ray emission is consistent with the existence of a preconditioning fast charge transfer. Both fast electrons having short lifetime and slow moving ions having long lifetime make a significant input into the charge transfer.

1. Introduction

Recent observations made by airplanes [14] balloons [3,4] and satellite-based detector [5] revealed the X-ray and gamma-ray flashes generated inside thunderstorm clouds. The generation of X-ray and γ-ray fluxes by thunderstorms has been attributed to bremsstrahlung of high energy electrons produced by the runaway breakdown [8,9,17]. The runaway breakdown is triggered by secondary cosmic-ray electrons, which are accelerated by the thunderstorm electric field, producing an avalanche of high energy electrons. The critical field for runaway breakdown is an order of magnitude less than the threshold of conventional air breakdown. Thus multiple runaway breakdown, triggered by cosmic rays develops during the preconditioning stage of a thunderstorm which precedes lightning flash. Besides, it develops on a scale length of order of tens or hundreds meters at normal atmospheric pressure.

The objective of this paper is to present a quantitative model of the X-ray generation inside thunderclouds due to the multiple runaway breakdown caused by the thunderstorm electric field. The model is based on the results of kinetic theory of the runaway breakdown. The X-rays propagation in the atmosphere, which is determined by the Compton scattering is considered. Comparison with the balloon observation [4] of the X-ray spectrum and intensity is provided, which shows a sufficient agreement between the theory and observations.

In the next section we present a model of multiple electron runaway breakdown caused by the thunderstorm electric field and compute the spectral density

* Corresponding author. E-mail: alex@td.lpi.ac.ru

0375-9601/99/$ - see front matter
PII: S0375-9601(99)00695-7

of the bremsstrahlung emission. In Section 3 we describe the X-rays propagation in the atmosphere affected by the Compton scattering, obtain the intensity and spectrum of the X-rays at different distances from the source and compare them with the observations made by Eack et al. [3]. It allows us to estimate the distance between the source and detector. In Section 4 we estimate the amount of electric charge transferred due to the multiple runaway breakdown, and compare the changes in the electric field caused by the above process with those observed in the thundercloud.

2. Model of multiple runaway breakdown

Presented here model of multiple runaway breakdown inside thundercloud triggered by cosmic ray secondary electrons is based on a following set of assumptions. Since a typical charge layer within the stratiform cloud has a horizontal extension of tens and more kilometers while its vertical thickness is a few hundred meters [15], we consider a one-dimensional model of the multiple electron runaway breakdown. Besides, the mean free path of both the high energy electrons and bremsstrahlung photons is much shorter than the atmospheric density scale, therefore we consider the atmosphere as uniform. We also assume that thunderstorm electric field causing the runaway breakdown is directed upwards. The collision frequency of runaway electrons is higher than electron gyrofrequency up to the height of 20 km [10], thus the runaway electrons inside a thundercloud can be treated as being unmagnetized.

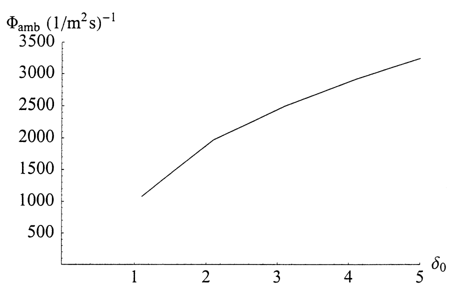

Fig. 1. Flux of cosmic secondary electrons which could trigger the runaway breakdown at corresponding electric field δ_0, computed for the height of 4 km.

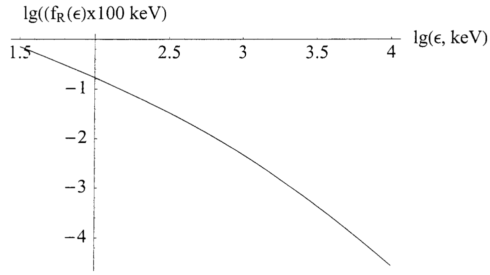

Fig. 2. The electron distribution function due to the runaway breakdown versus electron energy computed for $\delta_0 = 2.0$, and for the height of 4 km.

The runaway breakdown develops when the electric field exceeds the critical field [8]

$$E_c \simeq 2P(\mathrm{atm})\frac{\mathrm{kV}}{\mathrm{cm}}. \tag{1}$$

It is triggered by cosmic ray secondary electrons having the kinetic energy ε greater than ε_s, and injected at an angle θ to the electric field lesser than θ_s. Here ε_s and θ_s are determined by separatrix which separates the angle-energy space into two regions corresponding to the accelerating and decelerating electrons correspondingly [8,17].

The total flux Φ_{amb} of ambient cosmic ray secondary electrons involved in the runaway breakdown can be found by integrating the unidirectional differential intensity of cosmic ray secondary electrons $J(\mu,\epsilon)$ over the solid angle Ω and the energy range

$$\Phi_{amb} = \int d\Omega \int_{\epsilon_s(\mu,\delta_o)}^{\infty} J(\mu,\epsilon)\, d\epsilon. \tag{2}$$

Here $\mu = \cos\theta$, θ is the angle of the electron vector velocity to the electric field, while $\delta_0 = E/E_c$. The latter factor plays a critical role in the theory of runaway breakdown. Proceeding we assume based on the observations by Eack et al. [3], that the runaway breakdown occurs at 4 km, and adopt the values of the unidirectional differential intensity of cosmic ray secondary electrons from Fulks and Meyer [6] and Daniel and Stephens [2] we obtain the flux Φ_{amb} as a function of the electric field, which is shown in Fig. 1.

The runaway breakdown has been started by cosmic ray secondaries that produce an electron beam propagating downward along the vertical axis z, for a distance z_1 which corresponds to the thickness of the charge layer. As a result the flux of ambient cosmic ray secondary electrons will be magnified by the factor $\exp\{z/\ell_{\rm ion}\}$, where $\ell_{\rm ion}(\delta_0)$ is the characteristic ionization length for the exponential growth of the number of runaway electrons. Therefore the density of the runaway electrons is described by the following equation:

$$N_{\rm e}(z) = \Phi_{\rm amb} e^{z/\ell_{\rm ion}} \frac{1}{\beta c}, \quad \ell_{\rm ion} = c\beta\tau_i. \tag{3}$$

where $\tau_i(\delta_0)$ is the avalanche time, while $\beta(\delta_0) = v_{\rm s}/c$ is determined by the minimum velocity of the runaway electrons.

The bremsstrahlung intensity and spectra caused by the runaway electrons is determined by their electron distribution function $f_{\rm R}(\epsilon)$. The latter was first obtained by solving numerically the relativistic kinetic equation [17], and recently clarified by applying the proper ionization integral and boundary conditions [18] Using those results we present the electron distribution function obtained for $\delta_0 = 2$ and for the 4 km altitude by averaging over the different angles θ. Fig. 2 shows the electron distribution function normalized in such a way that $\int f_{\rm R}(\epsilon)\, d\epsilon = 1$ when integrating over the range of the runaway energy. Using this electron distribution function we compute next the spectral density I_ν of the bremsstrahlung emission

$$I_\nu = N_{\rm e} N_{\rm m} \int \sigma_\nu(\epsilon)\, v(\epsilon)\, f_{\rm R}(\epsilon)\, d\epsilon, \tag{4}$$

where $\sigma_\nu(\epsilon)$ is the cross-section for the production of photons in the frequency range $d\nu$ by the incident electron of energy ϵ. The latter is adopted from Kotch and Motz [13] for low electron energy $\epsilon < (2\text{–}3)mc^2$. Using Eq. (4) and taking into account the electron distribution function illustrated by Fig. 2,

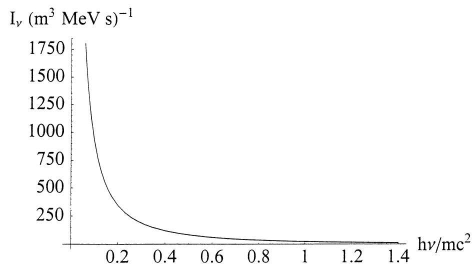

Fig. 3. Spectral density of the bremsstrahlung emission computed for $\delta_0 = 2.0$, and for the height of 4 km.

we obtain the spectral density of the bremsstrahlung emission. It is shown in Fig. 3 for the neutral density $N_{\rm m} = 1.5 \times 10^{19}$ cm^{-}3 which corresponds to a height of 4 km, and for a thickness of the charged layer $z_1 = 200$ m.

3. X-ray propagation in the atmosphere

The X-rays caused by bremsstrahlung of the runaway electrons propagate in the atmosphere from the source to detector. X-ray photons having the energy up to hundreds and even thousands keV experience Compton scattering by the atomic electrons. As a result, the photon energy gradually decreases, while its scattering cross-section increases. When the photon energy drops below 20–30 keV, they rapidly lost due to photoionization. Moreover, we consider the case when the photons propagate over a distance much shorter than the atmospheric pressure gradient scale, as well as and the horizontal extend of the source. Therefore the photon propagation is similar to 1D diffusion in the uniform atmosphere, which is described by the following equation:

$$\frac{\partial n}{\partial t} = D\frac{\partial^2 n}{\partial z^2} - \frac{\triangle\nu}{\lambda/c}\frac{\partial n}{\partial \nu} + Q(z,\nu). \tag{5}$$

Here $n(\nu,z,t)$ is the number of photons per cm^{-3} per frequency interval $d\nu$, and D is the coefficient of photon diffusion in the atmosphere due to the Compton scattering of cross-section $\sigma_{\rm c}(\nu)$

$$D(h\nu) = \frac{c}{N_{\rm m}\sigma_{\rm c}(h\nu)} \tag{6}$$

while $h\Delta\nu$ is the energy loss by the photon in a single collision, and λ is the mean free path of the photon

$$\lambda(h\nu) = \frac{1}{N_{\rm m}\sigma_{\rm c}(h\nu)}. \tag{7}$$

The mean energy losses and the Compton scattering cross-section have been described by Bethe and Ashkin [1]. Moreover we take into account that mean free path of the X-ray photons is longer than the characteristic ionization length for the exponential growth of the number of runaway electrons

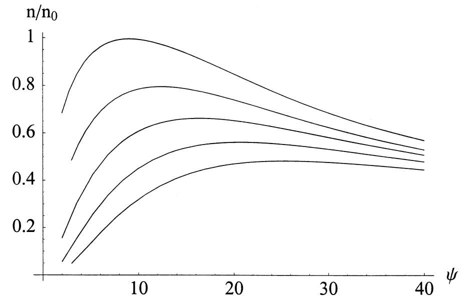

Fig. 4. Normalized photon spectral density n/n_0 versus $\psi(\nu)$ computed for different distances from the source. From top to the bottom the value of $\zeta-\zeta_0$ is equal to 0.05, 1, 2, 3, 4 respectively.

$(\lambda > \ell_{ion})$. Because of this most of the runaway electrons were born just before escaping the area filled with the intense electric field ($\delta_0 > 1$), in the layer of thickness ℓ_{ion}. Thus the X-rays source in Eq. (5) can be presented as a point source described by

$$Q = I_\nu \ell_{ion} \delta(z - z_0). \tag{8}$$

We consider then a stationary runaway discharge similar to that observed by Eack [4], and using dimensionless variables we present Eq. (5) in the following form:

$$\frac{\partial^2 n}{\partial\zeta^2} - \frac{\partial n}{\partial\psi} + \frac{N_m \sigma_c L^2}{c} Q = 0,$$

$$\zeta = \frac{z}{L}, \quad \psi = \int_0^\nu \frac{d\nu'}{\Delta\nu (N_m \sigma_c L)^2}. \tag{9}$$

Furthermore we chose L such that $L = 1/N_m Z \phi_0$, where $\phi_0 = 6.65 \times 10^{-25}$ cm^2 is the classical Thomson scattering cross-section [1] and Z is the mean molecular charge which is equal to 14.4 for air. Thus at 4 kilometer height $L = 70$ m. Solution of diffusion Eq. (9) with the source described by (8) is

$$n = \frac{N_m \sigma_c L \ell_{ion}}{c\sqrt{\pi}} \int_0^\psi \frac{d\psi'}{\sqrt{\psi - \psi'}} \times \exp\left\{ -\frac{(\zeta - \zeta_0)^2}{4(\psi - \psi')} \right\} I_\nu(\psi'(\nu)). \tag{10}$$

Eq. (10) was solved numerically by applying the source spectral density of the bremsstrahlung emission shown in Fig. 3. Result of those computation is illustrated by Fig. 4 which shows the normalized photon spectral density n/n_0 versus $\psi(\nu)$ computed for different distances from the source. Here we define the value n_0 as the maximum value of the curve $\zeta - \zeta_0 = 0.05$ which is reached at $\psi = 8$.

Since the source spectrum I_ν drops with ν while the photons mean free path increases with ν, the resulting photon spectral density peaks at a certain ν. Furthermore, at greater distances from the source this peak shifts to higher energies (or higher $\psi(\nu)$) due to increasing absorption, as revealed by Fig. 4.

Finally, in order to check our model by comparison against the spectrum observed by Eack [4] we compute the X-ray fluxes integrated over three energy channels 30–60 keV, 60–90 keV, and 90–120 keV. Each of those channels has different efficiency $\xi(k) = 0.94$, 0.88 and 0.69 for the channels $k = 1$, 2 and 3 correspondingly [4]. The total amount of photons observed per unit time by each of the detector's channels is

$$N_{tot}^k(\zeta) = \xi(k) \int_{\Delta\psi^k} n(\psi, \zeta) \frac{d\nu}{d\psi} d\psi \tag{11}$$

where $\Delta\psi^k$ is the width of the kth energy channel in the terms of ψ. From Eq. (11) we compute relative amount of X-ray photons collected by each of the above three channels of the X-rays spectrometer. This is shown in Fig. 5 obtained for different

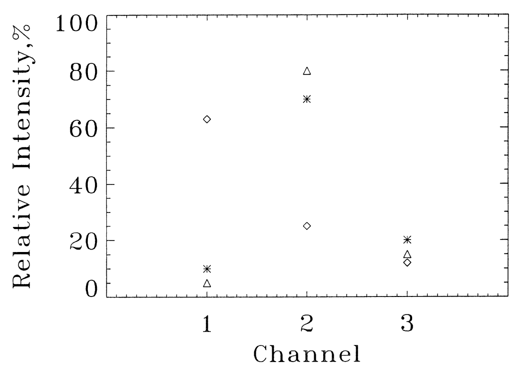

Fig. 5. Relative number of photons which could be received by each of three channels of the detector such as used by Eack et al. [3] at a different distances from the X-ray source. Diamonds correspond to computations at $\zeta = 1 (z = 70\,\mathrm{m})$, asterisks correspond to $\zeta = 6 (z = 420\,\mathrm{m})$, while triangles show real measurements by Eack et al. [3].

distances from the runaway discharge to the detector, along with the spectral observations [3]. Fig. 5 reveals that close to the photon source the low energy channel 1 dominates over the higher energy channels 2 and 3, while at larger distances from the source the channel 1 collects less photons than the channels 2 and 3, due to increasing attenuation. Comparison between the theory and observations allows us to determine the distance between the detector and runaway region which acts as the source of X-ray photons. This distance is about 400 m.

Based on the almost 1000 times increase of the background X-rays intensity observed by Eack [4] we can estimate from Eq. (3) the thickness of the charged layer as $z_1 \simeq 7\ell_{ion}$. Assuming $\delta_0 = 2$ we find that $\tau i = 167$ ns [18] while $\beta = 0.68$, thus Eq. (3) gives $z_1 \simeq 240\,\mathrm{m}$ which is consistent with a thickness of the charge layer of a few hundred meters as observed in thunderclouds by Marshall et al. [16].

4. Fast charge transfer

According to Gurevich et al. [8] fast electrons produced by the multiple runaway breakdown cause an intensive ionization of the air generating a large number of secondary electrons having low energies in the range of $\epsilon \sim 10$ eV. They rapidly loose their energy through inelastic collisions with air molecules, and becoming thermal electrons. The latter gradually disappear due to attachment to O_2 molecules, and in part to H_2O molecules followed by the conversion into heavy cluster ions. The electric charge is then transferred by both electrons and ions. Those processes are discussed below.

4.1. Electron charge transfer

Characteristic lifetime of free electrons in air at the altitude 4 km is about 70 ns [11]. During their lifetime the electrons are drifting under the action of the thundercloud electric field, which leads to a charge transfer. The drift is dominated by electron-neutral collisions, thus regardless of the direction at which electrons are emitted they drift along the direction of the electric field. Besides, the electron part of the fast charge transfer takes place till the free electrons generated by the runaway discharge exist. In our case the electric field is directed upwards, thus the electrons are moving downward providing the transfer of negative charge. Analysis of the electric field data obtained during the balloon flight through the thundercloud [3] allowed us to estimate the total charge transferred per unit surface of the clouds [11].

$$Q_1 \simeq 2 \times 10^{-4}\ \mathrm{C/m}. \tag{12}$$

From the other side, assuming that $\delta_0 = 2$, and taking the corresponding value of $\Phi_r(\delta_0 = 2)$, which then is multiplied by the magnification factor 1000, as discussed above, we obtain the flux of fast runaway electrons

$$\Phi_r \simeq 2 \times 10^6\ \mathrm{el/m^2\,s}. \tag{13}$$

This is consistent with estimates by Gurevich et al. [11]

Each of those runaway electrons creates about 50 low energy electrons along 1 cm of its trajectory, i.e. the ionization rate is $\eta \simeq 50\,\mathrm{el/cm}$. Since the slow electrons are produced along the distance $z_1 \sim 240\,\mathrm{m}$, their total flux is

$$\Phi_{sl} = \eta\, z_1 \Phi_r \simeq 2.4 \times 10^{12}\ \mathrm{el/m^2 s}. \tag{14}$$

Let us emphasize that in addition to high energy runaway electrons, related to the X-rays production, a significant input into the generation of thermal electrons is caused by less energetic electrons having a wide energy spectrum from about $\epsilon_c \sim 100$ keV down to the maximum energy needed per ionization of the air molecules $\epsilon_m \sim 110$ eV. Note that the effect caused by the less energetic electrons was not taken into account by Gurevich et al. [11]. Recent development in the kinetic theory of runaway breakdown shows that the electron distribution function grows appreciably in the low-energy range $\epsilon \leq 100$–$200\,\mathrm{keV}$. This leads to a significant increase in the ionization rate in comparison with ionization by runaway electrons only, given by a factor $\ln^2 \epsilon_c/\epsilon_m$ [12]

Therefore the total flux of slow electrons becomes equal to:

$$\Phi_{sl}^{tot} = \ln^2 \frac{\epsilon_c}{\epsilon_m}\, \Phi_{sl} \sim 50 \Phi_{sl}. \tag{15}$$

Furthermore consider the mean distance $l_d r$ traversed by the free electrons about 2.5 cm [11], and duration of the runaway breakdown process $t_{xr} \simeq 90$ s [3] we obtain that the charge transferred by electrons per unit surface is

$$Q = e\Phi_{sl}^{tot} t_{xr} l_{dr} \approx 10^{-4} \text{ C/m}. \quad (16)$$

This value is of the same order of magnitude as given by Eq. (12).

4.2. Ion charge transfer

Positive and negative ions produced by the runaway electron breakdown have long lifetime. Therefore they can transfer a significant amount of charge even when moving with a relatively low velocity. We estimate next the timescale of this process, and discuss the role of charge transfer by ions.

The temporal and spatial evolution of the electric charge carried by the ions eN_i is described by the following equations

$$\frac{\partial eN_i}{\partial t} + \nabla\sigma_i E = 0, \quad \nabla E = eN_i/\varepsilon_0, \quad (17)$$

where σ_i is the ion conductivity determined by the density of background quasi-neutral ion plasma $N_{i0}^+ = N_{i0}^- = N_{i0}$, and ε_0 is the permittivity of free space.

Assuming that $N_{i0} \gg N_i$ we find that

$$N_i = N_{i0}\,\mathrm{e}^{-t/\tau_i}, \quad \tau_i = \varepsilon_0/\sigma_i. \quad (18)$$

The ion conductivity is related to the average ion mobility μ_i by

$$\sigma_i = e\mu_i N_{i0}. \quad (19)$$

The average ion mobility in air is about 1.5 cm/Vs [7] Thus the characteristic relaxation time of the ion concentration found from Eqs. (18) and (19) becomes

$$\tau_i(s) \simeq 370\left[\frac{10^3}{N_{i0}(\text{cm}^{-3})}\right]. \quad (20)$$

A typical ambient ion plasma density in the air N_{i0} is about 10 cm^{-3} [7]. The ion plasma is created due to continuous ionization of air by the ambient flux of secondary cosmic-ray electrons.

In the runaway breakdown region the number density of fast electrons is growing up about three orders of magnitude. Consequently due to the effective ionization of air during runaway breakdown process and further attachment of thermal electrons to O_2 and H_2O molecules the number density of ions in a quasi-neutral ion plasma $N_i 0$ is growing up strongly – more than an order of magnitude. It became also height dependent $N_{i0} = N_{i0}(z)$, having maximum value in the vicinity of lower boundary of the runaway breakdown. The significant increase of N_{i0} leads to generation of ion currents which effectively reduce the thundercloud local electric charge according to Eqs. (18)–(20). Electric field height distribution in this region acquires then a specific flat-type form with the value $|E| < E_c$ been approximately constant. Note that the regions with characteristic flat-type maximum value of electric field (with $|E| < E_c$) have been observed in thunderclouds [15,4].

Acknowledgements

The authors express their appreciations to K. Zybin, M. Ptitsyn and J. Valdivia for valuable discussions. The work was supported by ISTC N490–96 grant, RBR grant N 98–02–10715, and NSF grant ATM 9713719.

References

[1] H.A. Bethe, J. Ashkin, in: E. Segre (Ed.), Experimental nuclear physics, vol. 1, Wiley, New York, 1953, pp. 166–357.
[2] R.R. Daniel, S.A. Stephens, Rev. Geophys. Space Phys. 12 (1974) 223.
[3] E.K. Eack, W.H. Beasley, J. Geophys. Res. 101 (1996) 29637.
[4] E.K. Eack, Rev. Sci. Instrum. 67 (1996) 2005.
[5] G.J. Fishman, Science 264 (1994) 1313.
[6] G. Fulks, P. Meyer, J. Geophys. 40 (1974) 751.
[7] W. Gringel, J.M. Rosen, D.J. Hofmann, in: E.P. Krider, R.G. Roble (Eds.), The Earth's Electrical Environment, National Academy Press, Washington, DC, 1986, p. 166.
[8] A.V. Gurevich, G.M. Milikh, R. Roussel-Dupre, Phys. Lett. A. 165 (1992) 463.
[9] A.V. Gurevich, G.M. Milikh, R. Roussel-Dupre, Phys. Lett. A 187 (1994) 197.
[10] A.V. Gurevich, J.A. Valdivia, G.M. Milikh, K. Papadopoulos, Rad. Sci. 31 (1996) 1541.
[11] A.V. Gurevich, G.M. Milikh, J.A. Valdivia, Phys. Lett. A 231 (1997) 402.

[12] A.V. Gurevich, K.P. Zybin, Phys. Lett. A 237 (1998) 240; A 243 (1998) 362.
[13] H.W. Kotch, J.W. Motz, Rev. Mod. Phys. 31 (1959) 920.
[14] M.P. McCarthy, G.K. Parks, Geophys. Res. Lett. 12 (1985) 393.
[15] T.C. Marshall, M.P. McCarthy, W.D. Rust, J. Geoph. Res. D 100 (1995) 7097.
[16] T.C. Marshall, M. Stolzenburg, W.D. Rust, J. Geoph. Res. D 101 (1996) 6979.
[17] R. Roussel-Dupre, A.V. Gurevich, T. Tunnel, G.M. Milikh, Phys. Rev. E 49 (1994) 2257.
[18] E. Symbalisty, R. Roussel-Dupre, S. Yakhymuk, IEEE Trans. Plasma Sci. 36 (1998) 2257.